LBL-20083
Preprint

Lawrence Berkeley Laboratory
UNIVERSITY OF CALIFORNIA

Accelerator & Fusion
Research Division

Submitted to Nuclear Instruments and Methods
in Physics Research

TRANSVERSE WAKEFIELD EFFECTS IN THE TWO-BEAM ACCELERATOR

F. Selph and A. Sessler

August 1985

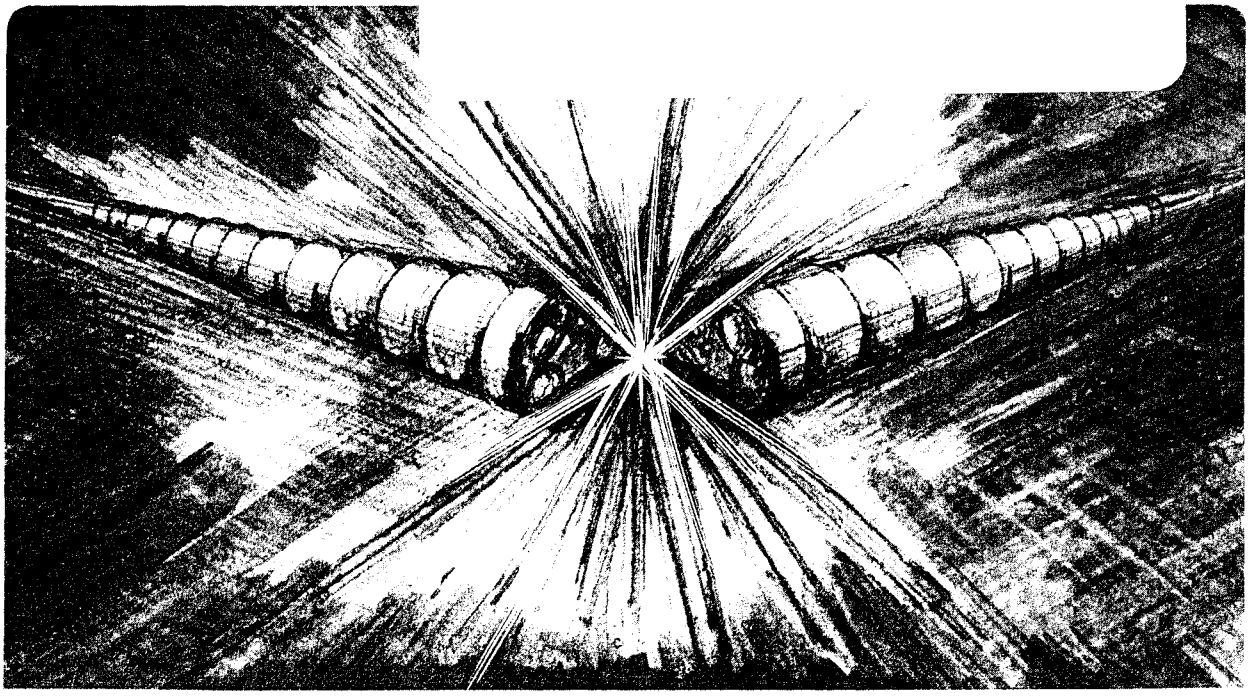

Prepared for the U.S. Department of Energy under Contract DE-AC03-76SF00098

LBL-20083

TRANSVERSE WAKEFIELD EFFECTS IN THE TWO-BEAM ACCELERATOR

Frank Selph and Andrew Sessler

Accelerator and Fusion Research Division
Lawrence Berkeley Laboratory
University of California
Berkeley, CA 94720

August 26, 1985

This work was supported by the Director, Office of Energy Research, Office of High Energy and Nuclear Physics of the U.S. Department of Energy under Contract No. DE-AC03-76SF00098.

TRANSVERSE WAKEFIELD EFFECTS IN THE TWO-BEAM ACCELERATOR*

Frank Selph and Andrew Sessler

Accelerator and Fusion Research Division
Lawrence Berkeley Laboratory
University of California
Berkeley, CA 94720

ABSTRACT

Transverse wakefield effects in the high-gradient accelerating structure of the Two-Beam Accelerator (TBA) [1-3] are analyzed theoretically using three different models. The first is a very simple two-particle model due to Wilson [4]; the second, due to Chao, Richter, and Yao [5], is for a beam with uniform charge distribution, constant betatron wavelength, and a linear wake approximation. Both of these models give analytic scaling laws. The third model has a Gaussian beam (represented by 11 superparticles), energy variation across the bunch, acceleration, variation of betatron focusing with energy, and variation of the wakefield from linearity. The three models are compared, and the third model is used to explore the wakefield effects when accelerator parameters such as energy, energy spread, injection energy, accelerating gradient, and betatron wavelength are varied. Also explored are the sensitivity of the beam to the wakefield profile and to the longitudinal charge distribution. Finally, in consideration of wakefield effects, possible parameters of a TBA are presented.

---

*This work was supported by the Director, Office of Energy Research, Office of High Energy and Nuclear Physics of the U.S. Department of Energy under Contract No. DE-AC03-76SF00098.

1. Introduction

When a point charge travels off axis in a linac structure, it generates a wake with transverse components that can deflect subsequent particles. This effect has been studied extensively for the Stanford Linear Collider (SLC). In this paper we extend some of these results for application to the Two-Beam Accelerator (TBA) [1-3].

In Section 2 we first describe a rather simple two-particle model studied by Wilson [4]. Second, we discuss a model studied by Chao, Richter, and Yao [5] in which a beam with uniform charge distribution, zero energy spread, and constant wavelength is subjected to a linearly varying wake. In sects. 3 and 4 we describe a model that proves useful for checking the first two, as well as for studying in more detail the effect of parameter variations, the effect of variation of wakefield shape, and the use of different charge distributions. The beam is represented by several superparticles, and a numerical solution of the equations is carried out on a computer. With this model, we can map the region of parameter space that is acceptable from the point of view of transverse wake effects. Finally, we give possible sets of parameters for the TBA.

2. Analytic formulas

2.1 The two-particle model

The simplest model of all is a two-particle model in which the first particle drives the second. Using this model, Wilson [3] obtains

$$R \equiv \left|\frac{x(L)}{x_o}\right| = \frac{NeLw_t}{4E_o k_\beta} , \qquad (1)$$

where x(L) is the amplitude of the transverse oscillations at longitudinal position L for an initial displacement x_o of the driving bunch, N is the number of electrons in a bunch, E_o is the energy of the bunch (assumed to be constant in this model), $k_\beta = 2\pi/\lambda_\beta$, where λ_β is the betatron wavelength (also assumed constant), and w_t is the wake caused by the first particle at the position of the second.

For the SLC, Wilson takes E_o to be the median energy of 25 GeV, $N = 5 \times 10^{10}$, $\lambda_\beta = 100$ m, $L = 3 \times 10^3$ m, and $w_t = 2.8 \times 10^{15}$ V/C/m^2. He then finds from eq. (1) that R = 10.

If the bunch has a spread of energies across it of magnitude ε, then Landau damping occurs, hence Wilson shows that

$$R = \frac{Newt}{2E_o k_\beta^2 \varepsilon} . \qquad (2)$$

This equation predicts that energy spread can be significant in reducing R: if $\varepsilon = 0.05$ and k_β is the same as before, we find the increase to be only 4.8; i.e., 2.1 times less than before.

2.2 The CRY model

The model of Chao, Richter, and Yao [5], which we will refer to as the CRY model, assumes a flat beam charge distribution, a linearly increasing wake behind a particle, and a constant betatron wavelength. If the beam is unaccelerated, i.e., of constant energy E_0 and with $\gamma_0 = E_0/mc^2$, they define a quantity

$$\eta \equiv \frac{r_0 L N W_0}{\gamma_0 k_\beta}\left(\frac{1}{2} - \frac{z}{\ell}\right)^2 , \tag{3}$$

where ℓ is the full length of a bunch, z is the distance measured forward from the center of the bunch, $r_0 = e^2/mc^2$, and the wakefield function W(z) is of the form

$$W(z) = W_0 z/\ell , \tag{4}$$

where W_0 is a constant. This function increases linearly. The wakefield function W(z) gives the force, eW(z), on a particle a distance z behind another of unit charge displaced by a unit amount. They next show for $|\eta| \gg 1$ that

$$R \equiv \left|\frac{x(L)}{x_0}\right| = \frac{\exp\left(\frac{3\sqrt{3}}{4}|\eta|^{1/3}\right)}{(6\pi)^{1/2}|\eta|^{1/6}} . \tag{5}$$

For the SLC, $W_0 = 5.9 \times 10^5\ m^{-3}$, and $r_0 = 2.8 \times 10^{15}$ m; taking $\gamma_0 = 5 \times 10^4$ (25 GeV), we find

$$\eta = 78.9\left(\frac{1}{2} - \frac{z}{\ell}\right)^2 . \tag{6}$$

Taking $z = \ell/(2\sqrt{3})$, i.e., one σ_z, we have $\eta = 49.1$, and hence $R = 14$.

If the beam is accelerated, then

$$\eta = \frac{r_0 L N W_0}{(\gamma_f - \gamma_i)k_\beta}\left(\ell n \frac{\gamma_f}{\gamma_i}\right)\left(\frac{1}{2} - \frac{z}{\ell}\right)^2 , \tag{7}$$

and

$$R = \left(\frac{\gamma_i}{\gamma_f}\right)^{1/2} \frac{\exp\left(\frac{3\sqrt{3}}{4}|\eta|^{1/3}\right)}{(6\pi)^{1/2}|\eta|^{1/6}} \quad . \tag{8}$$

For the SLC, $\gamma_i = 2.4 \times 10^3$ (1.2 GeV) and $\gamma_f = 10^5$ (50 GeV), so that

$$\eta = 146.95 \left(\frac{1}{2} - \frac{z}{\ell}\right)^2 \quad . \tag{9}$$

Taking $z = \ell/(2\sqrt{3})$, we have $\eta = 91.4$, and hence $R = 5.8$. Presumably, this is a better estimate than that given by the constant energy model, which is 14, or by the two-particle model, which gives 10. In any event, considering the approximations used here, these models can be considered to be in substantial agreement.

In recent work by Balakin and Smirnov [6], which extends the two-particle model, including energy spread, it is shown that for Landau damping to be most effective, the tail particle should have less energy than the head particle. Extending these ideas, Bane [7] shows that the Landau damping can exactly cancel the transverse wakefield force on the tail particle, provided a specific energy difference is maintained.

3. Numerical modeling of wakefields and focusing

3.1 Transverse wakefields

Transverse wakefields have been calculated for the SLC structure [4]. The magnitude of these fields is obtained by summing all harmonics. Fig. 1 shows the portion of the resulting wakefield function that is of interest in the present discussion. We want to scale this wakefield function to values appropriate to the TBA structures. The magnitude of the wakefields is pro-

portional to beam intensity and, according to Wilson, for structure parameters close to SLAC parameters, depends upon rf frequency and disk aperture as

$$w \propto \omega^3 a^{-3.5} . \tag{10}$$

The exponent of -3.5 for aperture scaling applies to the initial, positively sloping part of the curve at times < 20 ps; the magnitude of the curve as a whole scales as $a^{-2.25}$. However, as we will see in sect. 4.2, the asymptotic bunch behavior is dependent almost entirely upon the initial slope; thus we use the exponent of -3.5 as being more correct for our purposes.

The parameters of interest for wakefield scaling calculations are given in table 1 for the SLC and for several possible TBA structures operating at different frequencies. To scale values for the TBA structures from fig. 1, the bunch length relative to the rf wavelength needs to be taken into account. To do this for a given rf frequency ω and event time τ, we must read the wakefield amplitude w from the graph at a time

$$\tau_o = \tau(\omega/\omega_o). \tag{11}$$

It is convenient to treat the change in amplitude as a variable that is a function of both frequency and aperture and which will be denoted by S_c:

$$W = S_c w; \tag{12}$$

W is the wakefield amplitude (in GeV/m^2), and w is the amplitude given in fig. 1 (in picocoulombs per cell). Using the scaling relations of eq. (11), we find that S_c is given by

$$S_c = 2.0 \times 10^{-2} \left(\frac{\omega_o}{\omega}\right)^{0.5} \left(\frac{a_o}{a}\right)^{3.5} \frac{N}{N_o} . \tag{13}$$

In this formula, ω is the new frequency, a the new disk aperture, N the new beam intensity; ω_o and a_o are SLC parameters given in table 1, and $N_o = 5 \times 10^{10}$. Note that in eq. (13) S_c is proportional to N. In fact, we

use the computer calculation described in sect. 4 to find the value of S_c that will give a maximum allowable beam displacement; then eq. (13) can be used to find N.

3.2 Betatron wavelength

The strength of the wakefields is proportional to the displacement of the exciting particle from the axis. This leads to the requirement that quadrupole focusing needs to be strong in order to minimize betatron amplitudes. An estimate of achievable betatron wavelengths for a linac of 1 TeV is given in fig. 2. The curve labeled $F_\lambda = 35$ requires quadrupoles of maximum strength 600 T/m; that labeled $F_\lambda = 20$, about 1000 T/m. The former would have a 4 mm aperture, the latter a 2 mm aperture. A transport system is assumed, using quadrupoles with permanent magnets similar to a design proposed by Halbach [8]. To date such magnets have been made only with apertures on the order of a centimeter in diameter, but the design appears to be suitable for smaller apertures. A practical limiting factor in the focusing strength is the proportion of the linac length devoted to quadrupoles; here it is taken as 10%. It may be possible to have the focusing quadrupoles around the high-gradient structure (a dual use of space), thus saving accelerator length.

4. Calculations and results

4.1 Differential equation for calculation of wakefield effects

The bunch is represented by 11 superparticles with a Gaussian charge distribution extending from $-2\sigma_z$ to $2\sigma_z$. The fraction of charge assigned to each particle is given in table 2.

The differential equation for the i^{th} particle can be written

$$\frac{d}{dz}\left(\gamma_i(z)\frac{dx_i}{dz}\right) + \gamma_i(z)k_\beta^2(z)x_i = F_i \ , \tag{14}$$

where

$$F_i = \sum_{i>j} M_{ij}x_j \ . \tag{15}$$

The symbol F_i represents the forces acting on the i^{th} particle from particles downstream. It is assumed that particles are traveling close to the speed of light, so that wakefields from particles upstream of the i^{th} particle will not be able to influence it. The strength of the wakefield M_{ij} acting on the j^{th} particle depends upon x_j, the displacement of the j^{th} particle, as well as its charge.

If ε represents the maximum energy spread of the bunch and G the energy gain per meter, then ε_i, the energy fraction of the i^{th} particle, is

$$\varepsilon_{i\pm} = 1 \pm \frac{(i-1)}{10}\,\varepsilon \ , \tag{16}$$

and the energy of the i^{th} particle is

$$\gamma_i = \varepsilon_{i\pm}(\gamma_0 + Gz) \ . \tag{17}$$

The plus sign results in increasing energy from head to tail, the minus sign in decreasing energy from head to tail. We will use both in our calculations to determine which will be best for Landau damping. Setting $k_{\beta i} = 2\pi/\lambda_{\beta i}$, where $\lambda_{\beta i}$ is the betatron wavelength at the i^{th} particle, the focusing term can be written as

$$Q = \frac{(2\pi)^2(\gamma_0 + Gz)}{\lambda_{\beta i}} \ . \tag{18}$$

Collecting terms and rearranging, eq. (15) becomes

$$\frac{d}{dz} x_i' = \frac{1}{\gamma_i}(F_i + Gx_i' - Qx_i) \ , \tag{19}$$

which is the differential equation that will be used to solve for x_i and $x_i' \equiv dx_i/dz$ as a function of z.

4.2 Computer calculation of wakefield effects

At the start of a calculation, all 11 superparticles (SP) are displaced by the same amount x_0. As the calculation proceeds, each SP will undergo betatron oscillations while contributing to the wakefields in proportion to its displacement at that instant. Fig. 3a shows the displacement of the SP as the bunch is accelerated. Here maximum relative displacements R, where we let $R \equiv |x_{max}|/x_0$, are plotted for each SP at 500 GeV. At the start, R = 1 for all SP. Note that as acceleration proceeds, the particles near the head of the bunch are relatively unaffected by the wakefields but are damped by the increase in energy. Toward the tail of the bunch, particles are strongly affected by the wakefields. However, the tail contributes relatively little to the bunch (see table 2). A more balanced picture is shown in fig. 3b, which gives plots of displacement weighted by the charge fraction q_i of each SP. Two plots are shown for positions one-half betatron wavelength apart. Note that the maximum weighted displacement occurs for SP 8 and that the wakefield forces in this case cause the tail particles to oscillate out of phase.

In order to get some idea as to the importance of the form of the charge distribution used, calculations were performed using two radically different distributions: (1) the Gaussian distribution of table 2 and (2) the flat distribution. The results are plotted in fig. 4. The most striking thing about these plots is that although the tail particles show greater weighted displacement, as expected, the phases are the same for each distribution. The plots are made for the same distance along the accelerator.

To compare the wakefield effect for different accelerator parameters, the quantity R was calculated as a function of position along the accelerator, and $|x_{max}|$ was taken as the absolute maximum displacement of SP 1 through 8 from the axis. Particles 9-11 in the tail of the bunch were excluded, because in a Gaussian distribution the amount of charge they represent is small.

For comparison with the estimates of sect. 2, the program was used to calculate R for the SLC parameters (table 1) for two cases: $\varepsilon = 0$ and $\varepsilon = 0.05$ (using the ε_{i-} formula). The relative displacement of R agrees well with the analytic calculation of the CRY model (eq. 8), which predicts R = 5.8 for the case $\varepsilon = 0$. The CRY model does not include the effect of energy spread, but Wilson's two-particle model (eq. 2) does predict Landau damping by a factor of 2 at 50 GeV. Although the computer model shows less damping, it is still substantial. Bane [7] has carried out extensive computer studies for the SLC case and shows that with "fine tuning" of the energy spread, the relative displacement R can be reduced by a much larger factor.

We wanted to get some idea of the general behavior to expect from Landau damping in a TBA of 1 TeV. As a first step, calculations were done using the two energy spread functions ε_{i+} and ε_{i-}. If the predictions of refs. [6] and [7] are correct, we expect that ε_{i-} will be much more effective in producing damping. This indeed turned out to be the case, as can be seen in fig. 5. Both runs were made with the same wakefield function scaled for TBA1, the 28 GHz case, with $\varepsilon = 0.2$. The calculation done with ε_{i+} shows a uniform growth in R, reaching a maximum at 1000 GeV. The ε_{i-} calculation shows strong Landau damping. Note that the intensity here was chosen to be 6 times larger than for the ε_{i+} case; this choice is responsible for the initial steep uniform growth

in R to a value of about 55 before the damping sets in around 70 GeV. At that energy a very strong and sudden decrease in R occurs, and R remains below 5 from 200 to 1000 GeV.

Fig. 6 shows R as a function of negative ε_{i-} energy spread. The reduction of R is relatively small at low energies, but at higher energies there is a substantial reduction in R for all values of ε. At 1000 GeV the reduction in R is 290 times, from $\varepsilon = 0$ to $\varepsilon = 0.1$.

The allowable increase of intensity with increasing energy spread was examined for the TBA1 parameters. In these calculations the maximum allowable value for R was taken as 20 at energies above 500 GeV. The result is that with ε_{i-} less than about 5%, intensity N is limited to about 10^{10} particles per bunch. With larger energy spread, N increases sharply up to an energy spread of 20%, where $N = 10^{11}$. For a collider, use of energy spreads as large as 20% will clearly need to be considered for experiments that require highest intensity.

Variation of R with injection energy is not clearly evident when strong Landau damping is present. However, if we look at runs without such damping, with a ε_{i+} energy spread, then as injection energy is varied X varies roughly proportional to $\gamma_i^{1/2}$. This is in substantial agreement with eq. (8). Thus a relatively low injection energy would seem to be a good choice, other factors being equal.

The effect of varying focusing strength is shown in fig. 7. The corresponding betatron wavelengths that were used are shown in fig. 2. Clearly, strength of focusing is an important parameter. In this calculation the curve labeled $F_\lambda = 20$ requires quadrupoles with strengths on the order of 1000 T/m.

Fig. 8 shows the effect of varying acceleration gradient. For gradients G of 0.25 GeV/m to 0.6 GeV/m, relative amplitude R is reasonably small near 1000 Gev. This is most important in order to maximize luminosity for a collider. The peak that occurs below 100 GeV will limit transmitted intensity unless a way can be found to lower it to, say, 20. It is possible that this might be done with some "special tuning" of the energy spread and gradient in this region. Clearly, however, a high gradient, about 0.5 GeV/m, is preferred. The TBA gradients are expected to be in the range of 0.3 to 0.6 GeV/m.

Because the shape, as well as the magnitude, of the wakefield function can vary considerably, it is a matter of some importance to know just how sensitive the relative amplitude R is to variations in the shape of the W function. To explore this point, a number of different wakefield functions were tested, the object being to choose a scaling factor S_c for each, so that at 1000 GeV the result would be R = 20 in each case. The resulting values for these wakefield functions are shown in fig. 9. The most striking feature of these functions is that the detailed shape of their curves varies greatly, but they all have the same value W = 10.5 in the vicinity of SP 2 and 3. The displacements R converge to R = 20 at 1000 GeV and are remarkably similar at lower energies. In particular, although the wakefields associated with functions (a) and (c) are widely different except in the region of SP 2-4, the R values lie so close together that they can be represented by the same curve, except for a small difference near 300 GeV.

A conclusion that can be drawn from this exercise is that the detailed shape of the wakefield function is not particularly important. What is important, however, is establishing the strength of wakefields near the head of the bunch.

To summarize some of the results, we present parameters in table 3 of two TBA cases worthy of future study. The frequencies chosen are 28 and 17 GHz; the corresponding scaled wakefield functions are given in fig. 9 as (a) and (b). To achieve the intensities shown in table 3, some means will need to be found to reduce R in the region below 300 GeV. This may be made possible by "fine tuning" the energy spread and the accelerating phase.

Appendix: Note on comparison of CRY formula with computer calculations

As an insight into the predictive potential of the CRY formula (eq. 8), we undertook to make a comparison of the quantity R with computer calculations of R at 1000 GeV. Injection energy was taken as 2 GeV, energy spread as $\epsilon = 0$, and accelerating gradient as 0.5 GeV/m. The constant W_o is proportional to S_c; for $S_c = 1$, W was taken as 2.95×10^7. There remain a number of discrepancies between the two calculations:

1) CRY uses a flat charge distribution; the computer calculation uses a Gaussian.
2) CRY uses a linearly increasing W function; the computer calculation uses a scaled SLC function w_1.
3) CRY uses a constant λ_β; the computer calculation uses a curve close to $F_\lambda = 35$, shown in fig. 2.

Note, however, that there are no free parameters in either the CRY formula or in the computer runs. Results are plotted in fig. 10, showing R as a function of S_c. Considering the discrepancies in the input parameters mentioned above, the agreement is remarkable. Noteworthy is the fact that the two curves have the same slope. The slope is very steep, suggesting that as S_c (which is proportional to intensity) is increased, the onset of beam blowup is sudden.

References

[1] A.M. Sessler, in: Laser Acceleration of Particles, AIP Conference Proc. No. 91 (American Institute of Physics, 1982), pp. 154-159.

[2] D.B. Hopkins, A.M. Sessler, and J.S. Wurtele, Nucl. Instr. and Meth. 228 (1984), 15-19.

[3] F.B. Selph, AIP Conference Proc. No. 127, High Energy Particle Accelerators (BNL/SUNY, Stony Brook Summer School, 1983) pp. 929-946.

[4] P. Wilson, in: AIP Conference Proc. No. 87, eds., R.A. Carrigan, F.R. Huson, and M. Month (American Institute of Physics, 1982), pp. 450-558.

[5] A.W. Chao, B. Richter, and C.Y. Yao, Nucl. Instr. and Meth. 178 (1980), 1.

[6] V.E. Balakin and A.V. Novokhatsky, Proc. of 12th International Conference on High Energy Accelerators (Fermi National Accelerator Laboratory, 1983), pp. 119-120.

[7] K.L.F. Bane, Proc. of 1985 Particle Accelerator Conference, Vancouver, B.C., Canada (May 1985); also Stanford Linear Accelerator Center SLAC-PUB-3670 (April 1985).

[8] K. Halbach, Jour. Appl. Phys. 57 (1985), 3605-3608.

Table 1

Parameters used for scaling transverse wakefields

	SLC	TBA1	TBA2	TBA3
rf frequency $\omega/2\pi$ (GHz)	2.856	28.0	21.0	17.0
Aperture radius a (mm)	11.600	2.0	3.0	3.9
Bunch length (mm)	1.000	1.0	1.0	1.0

Table 2

Charge distribution on superparticles (SP)

SP	Charge ratio
1, 11	0.022
2, 10	0.045
3, 9	0.078
4, 8	0.116
5, 7	0.147
6	0.159

Table 3

Parameters for two TBAs

	TBA1	TBA3
rf frequency (GHz)	28.0	17.0
Aperture radius a (mm)	2.0	3.9
Beam length σ_z (mm)	1.0	1.0
Betatron wavelength function F_λ	30.0	30.0
Injection energy (GeV)	1.0	1.0
Accelerator gradient (GeV/m)	0.5	0.5
Energy spread ϵ	0.2	0.2
R near 1000 GeV	20.0	20.0
Intensity N	1.1×10^{11}	1.4×10^{11}

Figure Captions

Fig. 1. Transverse wakefield function calculated for SLC by Wilson [4]. By scaling this function with frequency, aperture, and intensity, estimated wakefields are found for the TBA calculations reported here. The calculations demonstrate that although the scaling is not likely to be exact, the detailed shape of the curve is not important in calculating wakefield effects.

Fig. 2. Betatron wavelengths used in the calculations. To minimize wakefield effects, λ_β should be small. Here it is assumed that no more than 10% of the linac structure is taken up with quadrupoles. The curve labeled F = 35 assumes a 4 mm quadrupole aperture; the curve F = 20, a 2 mm aperture.

Fig. 3. Typical particle displacements along the high-gradient structure. The greatest displacements are toward the tail of the bunch. (a) Typical SP displacements, here shown at 500 GeV. All SP have R = 1 at the start. (b) Charge-weighted displacements, here shown at points one-half betatron wavelength apart.

Fig. 4. Results of calculations in which the same structure parameters but different charge distributions were used. The ordinate is the SP displacement weighted with the charge fraction. (a) Gaussian charge distribution of Table 2. (b) Flat charge distribution.

Fig. 5. Comparison of the Landau damping between "positive" (ε_{i+}) and "negative" (ε_{i-}) slope, head-to-tail, of energy spread (see eq. 17). Energy spread in both cases was $\varepsilon = 0.2$. The contrast between positive and negative slope is much greater than the figure suggests, because N for the ε_{i-} case was 6 times greater than for the ε_{i+} case: for ε_{i+}, $N = 1.1 \times 10^{10}$; for ε_{i-}, $N = 6.7 \times 10^{10}$.

Fig. 6. Maximum particle displacement R as a function of "negative" energy spread ε_{i-} and final energy, with $N = 10^{10}$.

Fig. 7. Variation of R with focusing strength, using betatron wavelength functions of fig. 2. Both calculations used parameters of TBA1 (see table 1), with $N = 7 \times 10^{10}$, $\varepsilon = 0.2$ with "negative" slope.

Fig. 8. Variation of R with acceleration gradient G. TBA1 parameters: $N = 5 \times 10^{10}$, $\eta = 0.2$ with "negative" slope. For a TBA, G is expected to be in the range 0.3-0.6 GeV/m. (a) The maximum value of R in the range below 100 GeV, where Landau damping is not yet effective. At G = 0.25, R = 107 (off scale). Special tuning measures might be effective in reducing R in this region. (b) Maximum R in the range 900-1000 GeV, which is of most interest for a 1 TeV collider.

Fig. 9. Several wakefield functions that produce a value of R = 20 at 1000 GeV. (a) Function W scaled from fig. 1 for parameters of TBA1, with S_c = 6.6. (b) Function W scaled from fig. 1 for parameters of TBA3, with S_c = 7.6. (c) W is flat, the same for all SP. (d) W as a linearly increasing function, as in eq. (4). The only feature that these curves have in common is that they all have similar values in the vicinity of SP 2 and 3. This leads to the conclusion that the strength of the wakefields near the head of the bunch is the most important feature determining particle behavior.

Fig. 10. Comparison of CRY formula (eq. 8) with computer calculations at 1000 GeV. There are no free parameters in either calculation; see text for details. (a) CRY formula. (b) Computer calculation. These results suggest that the CRY formula can be relied upon to give a useful estimate of wakefield effects.

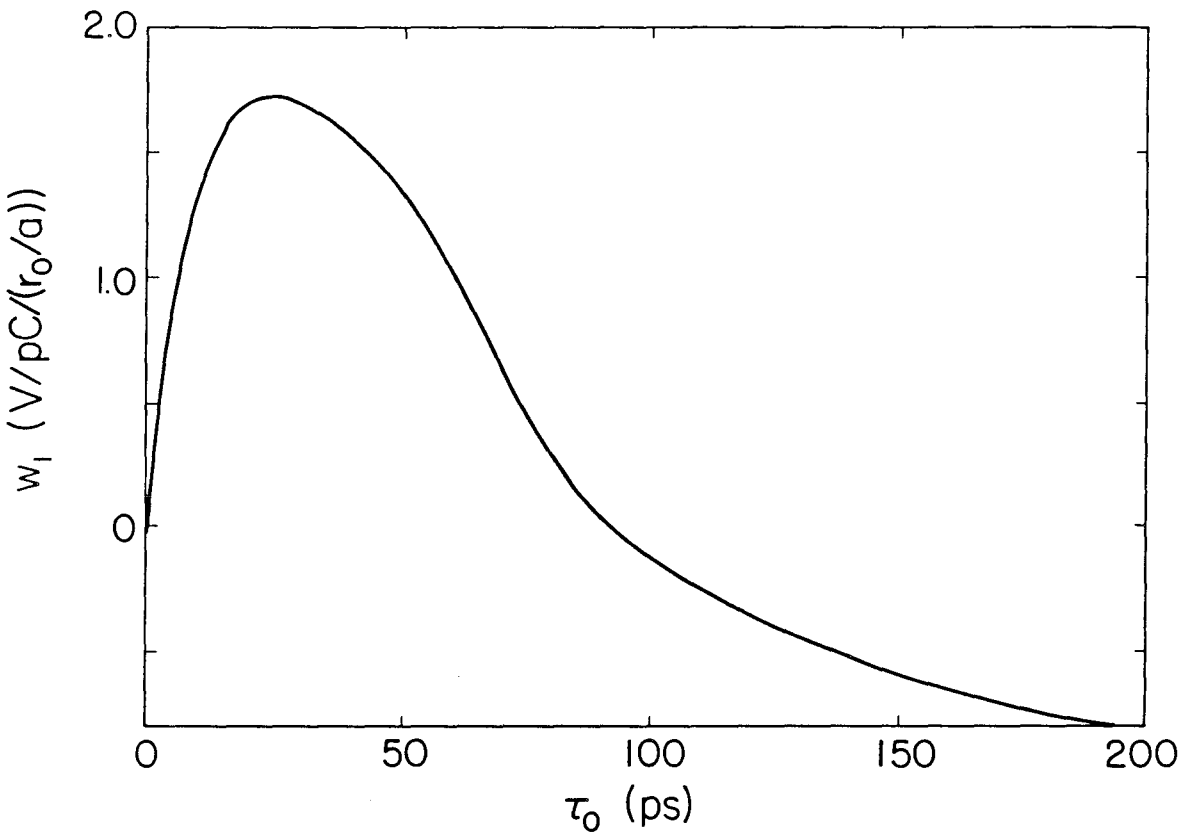

XBL 858-10683

Fig. 1

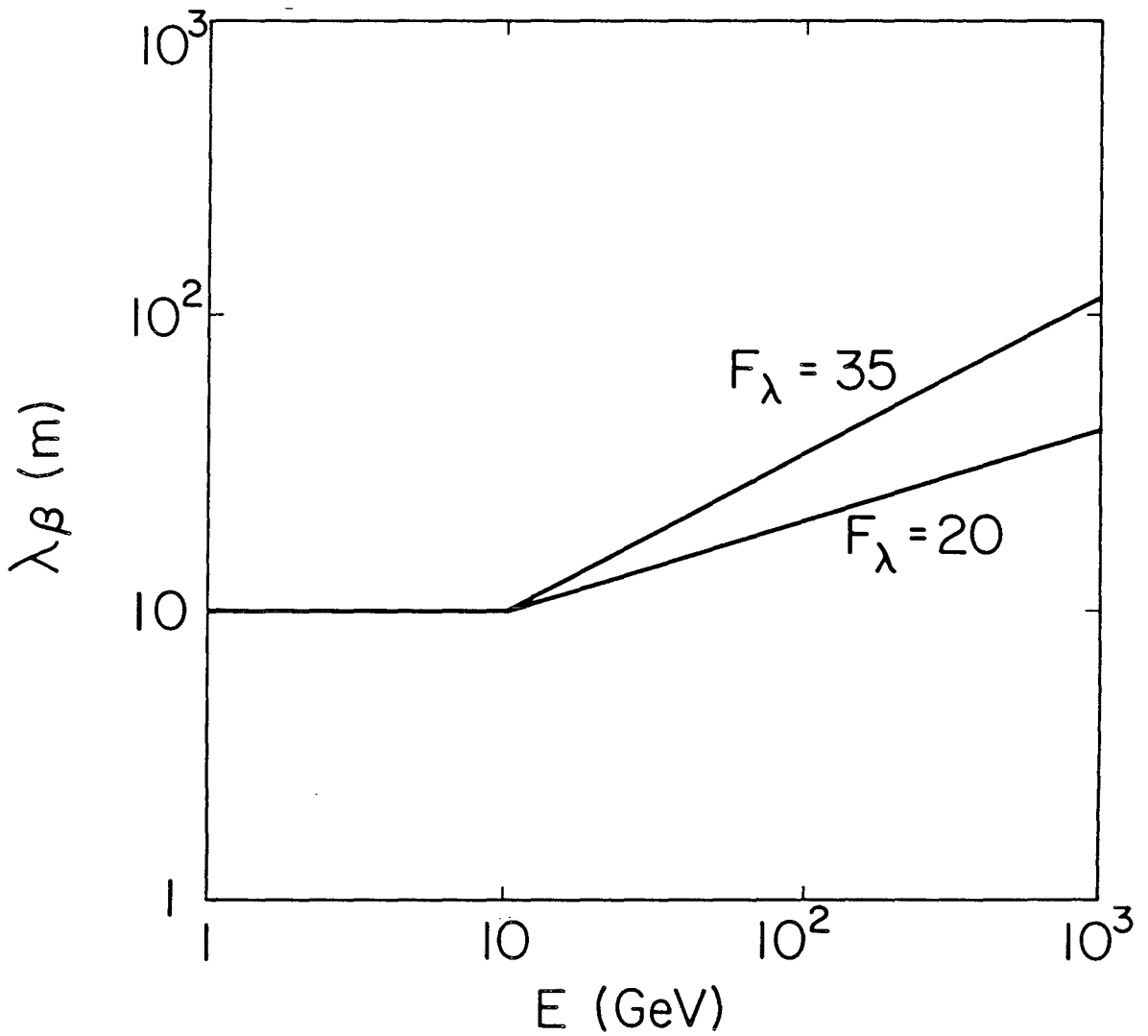

XBL 858-10684

Fig. 2

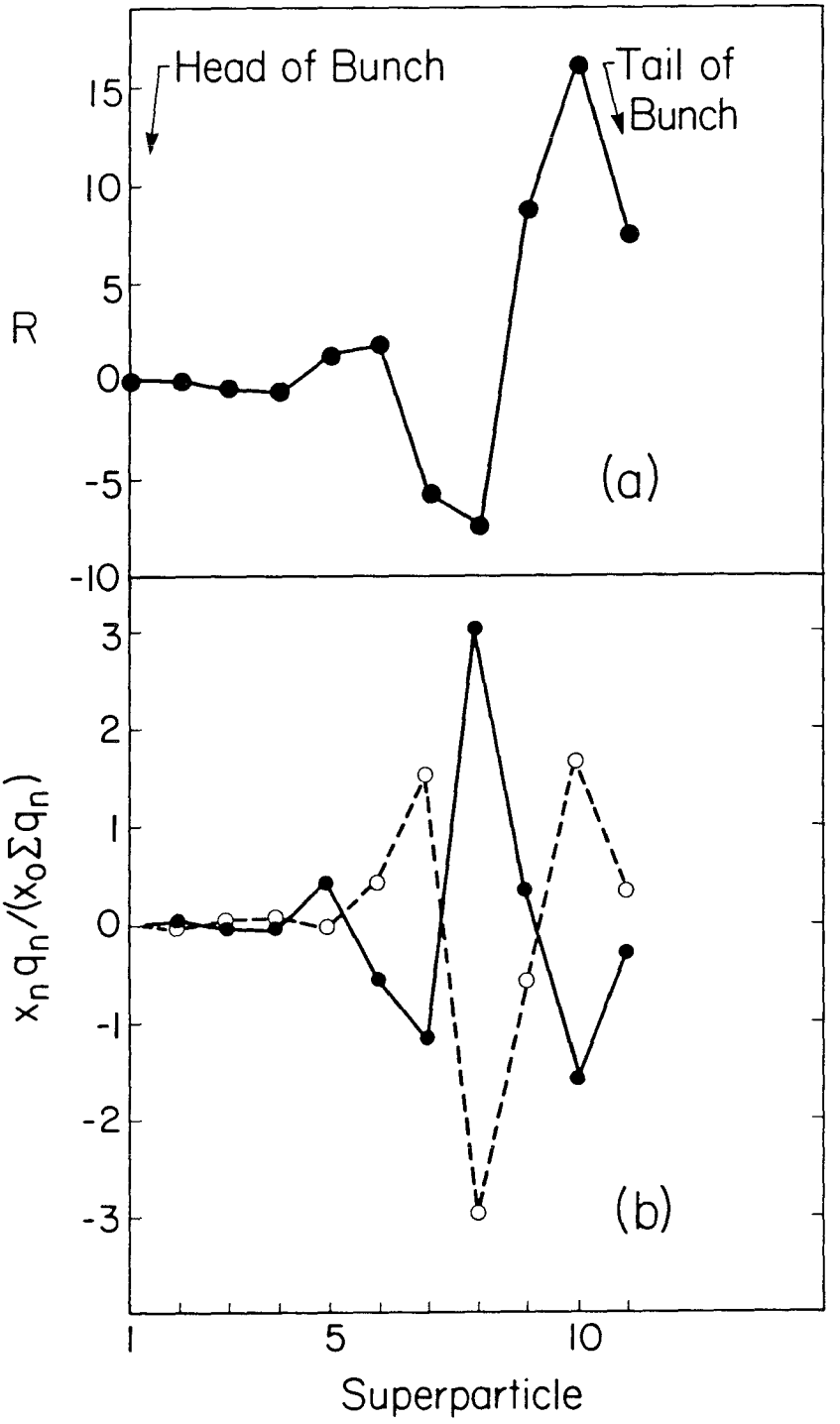

XBL 858-10687

Fig. 3

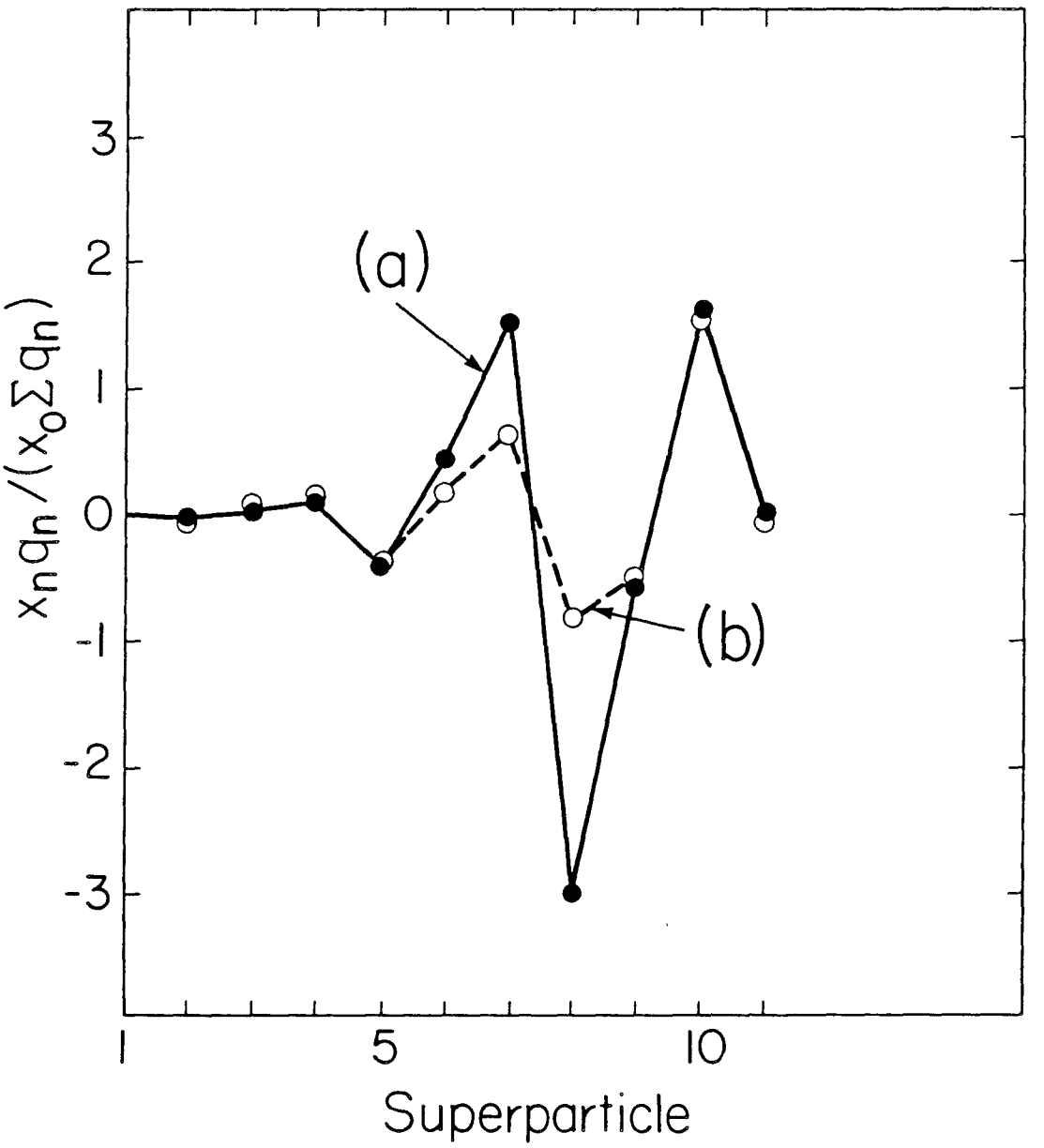
3
2
1
0
-1
-2
-3
(a)
(b)
$x_n q_n / (x_o \Sigma q_n)$
1
5
10
Superparticle
XBL 858-10688

Fig. 4

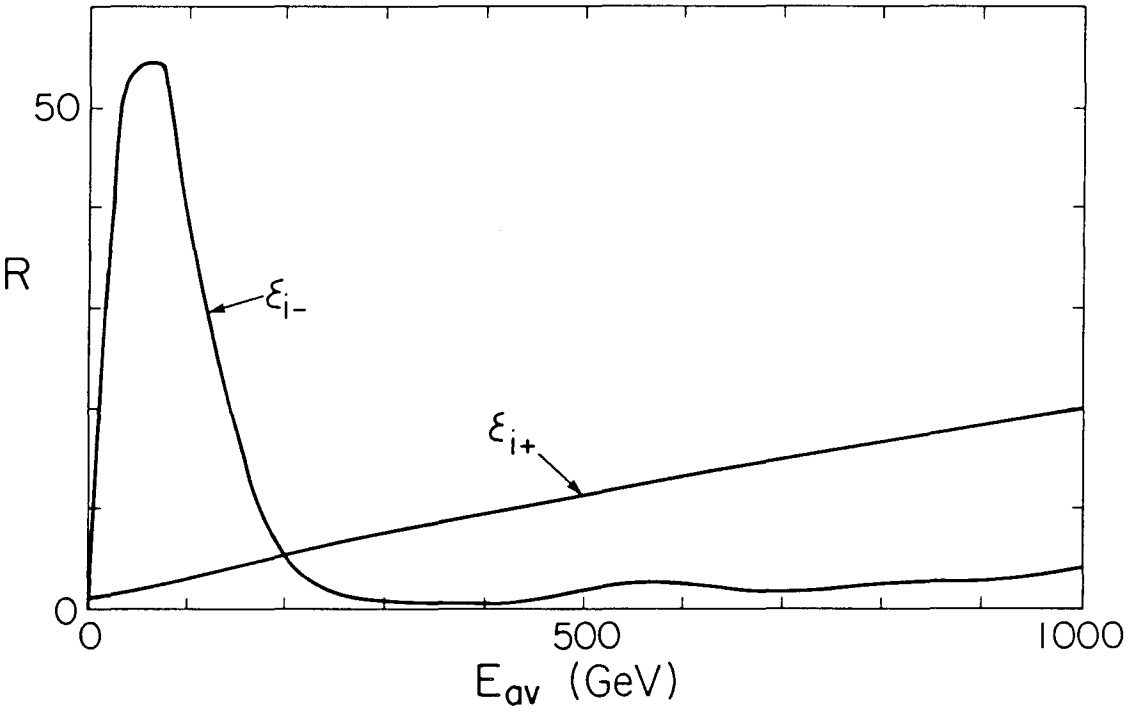

XBL 858-10690

Fig. 5

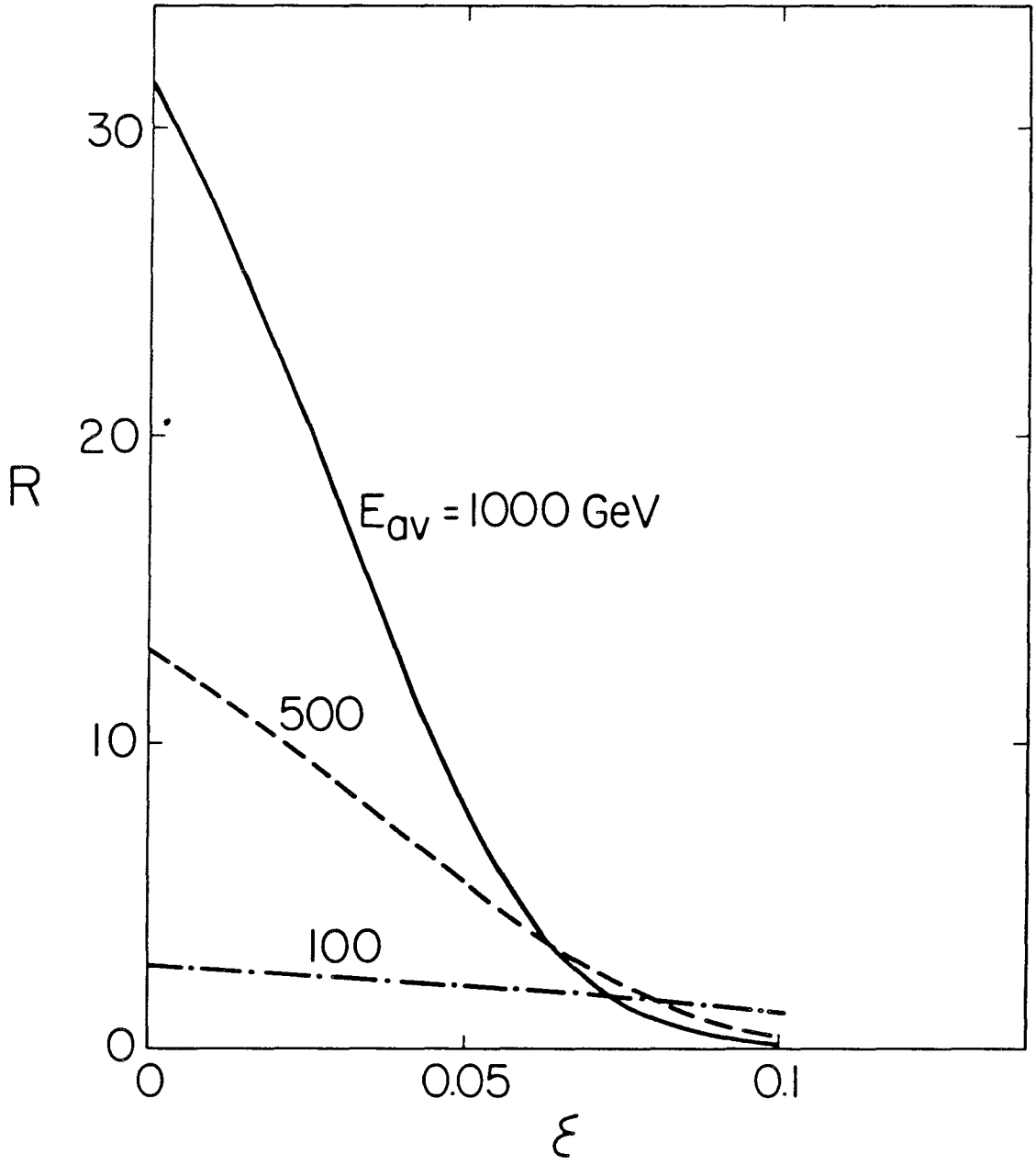

XBL 858-10692

Fig. 6

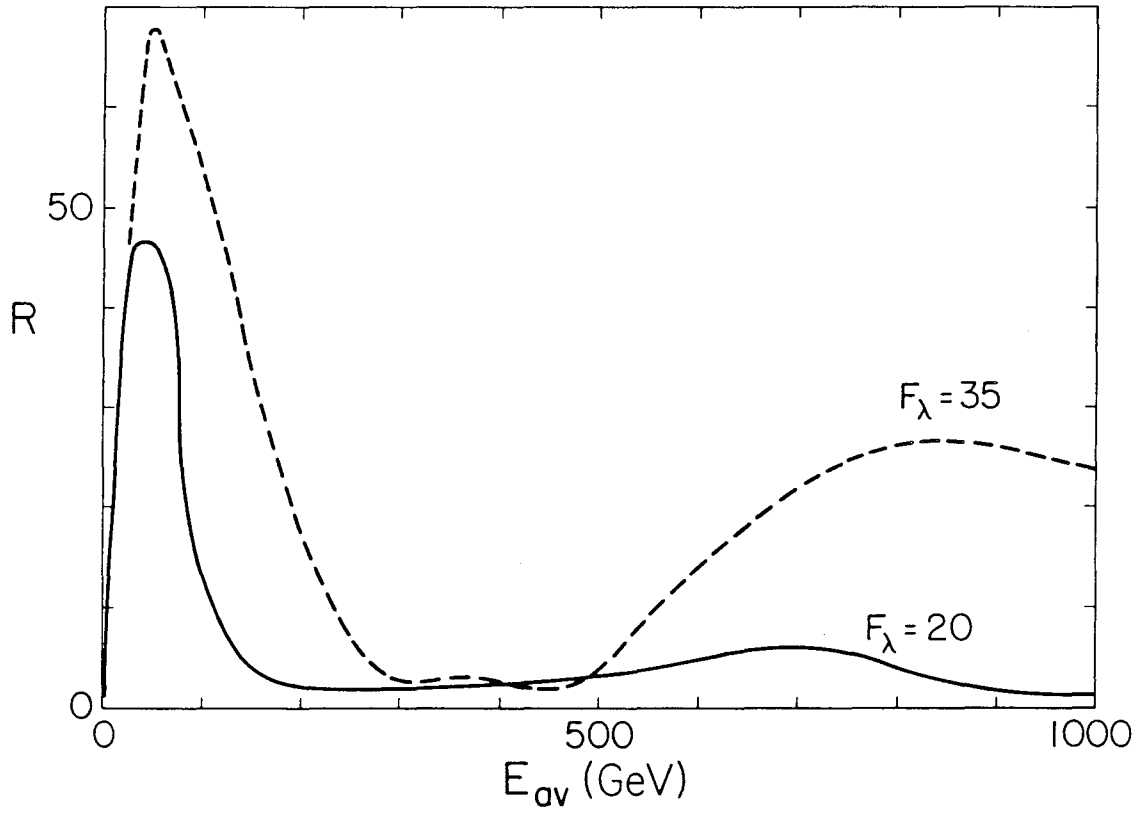

Fig. 7

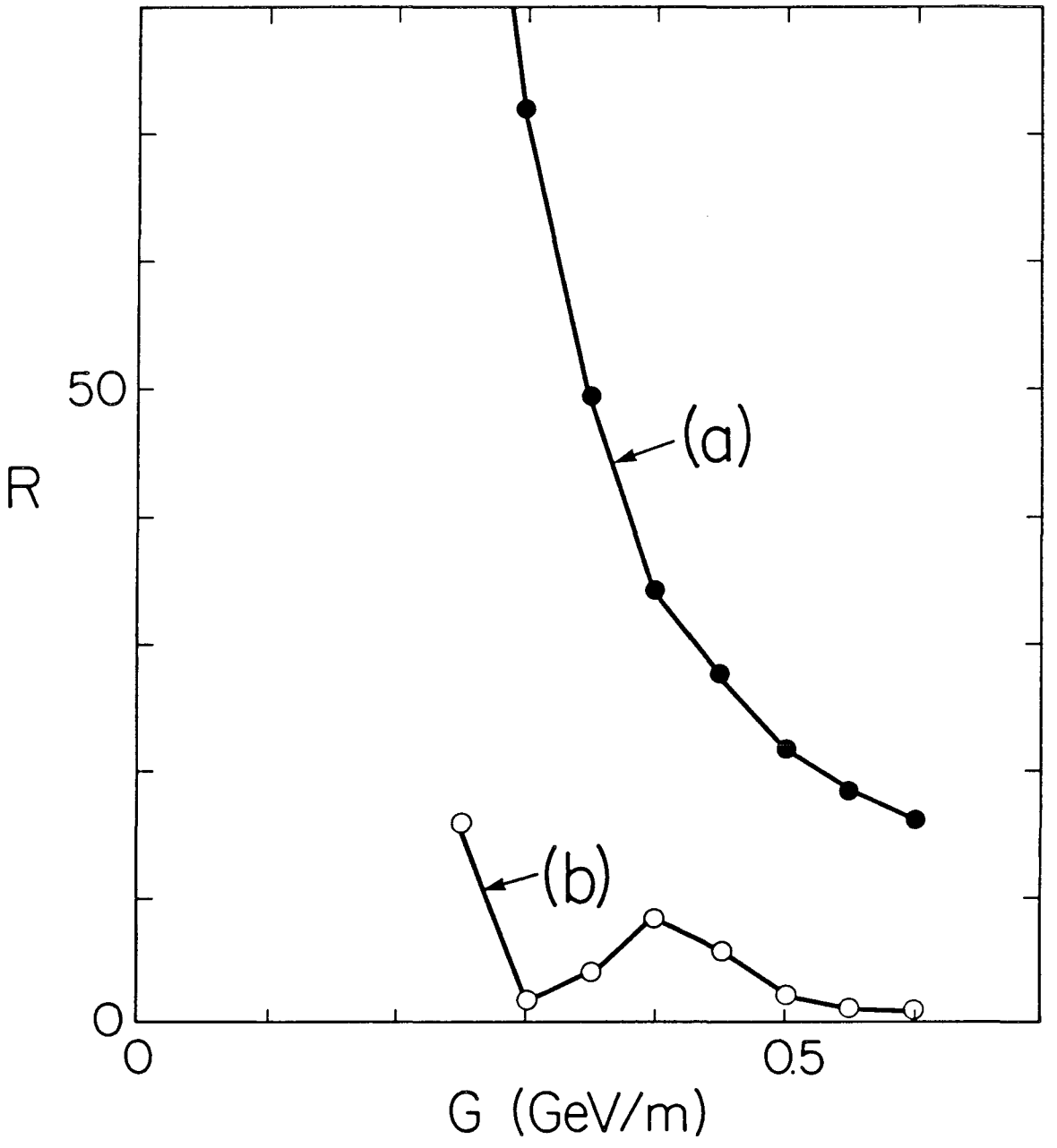

XBL 858-10696

Fig. 8

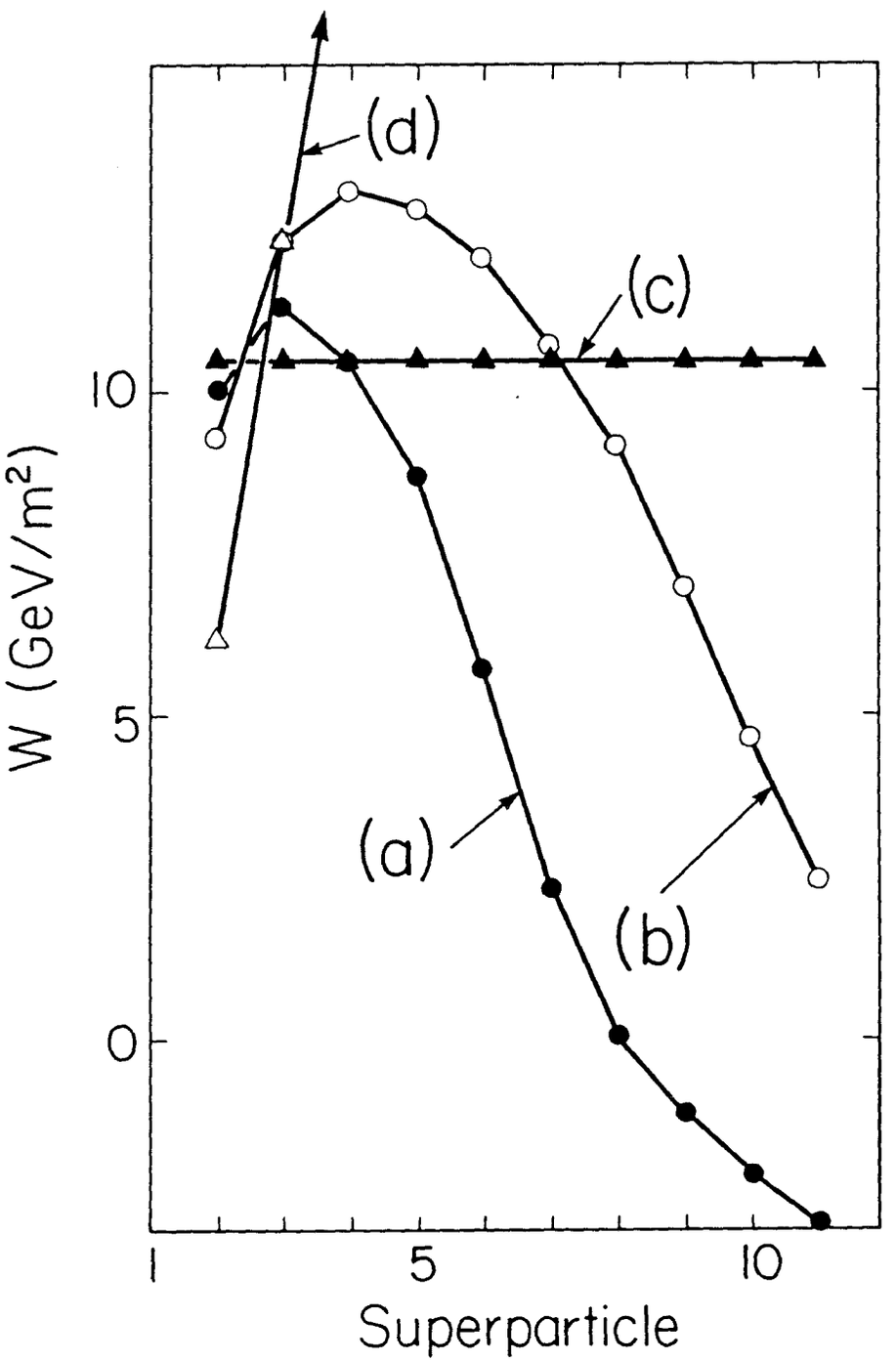

Fig. 9

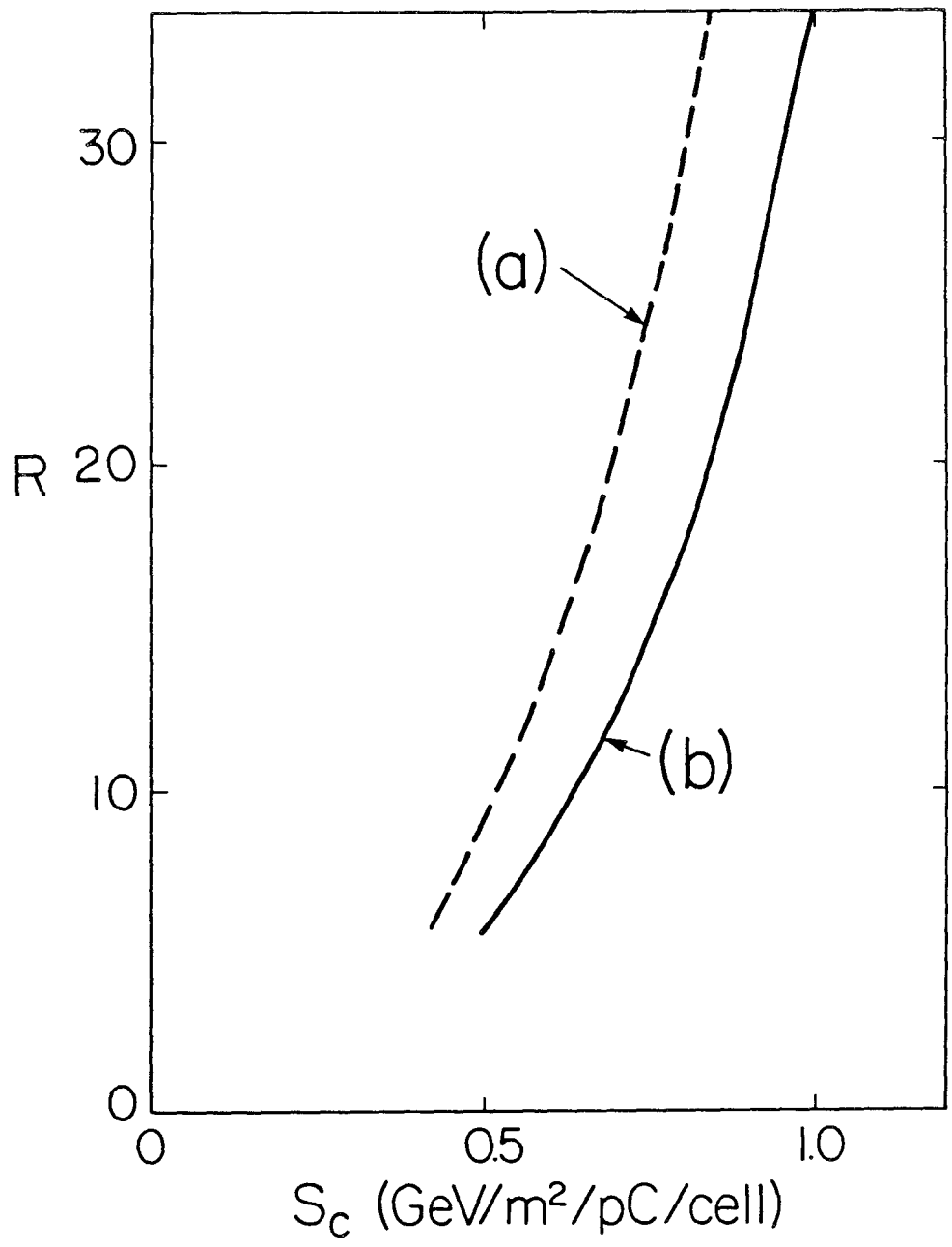

XBL 858-10699

Fig. 10